

Auxiliary-Bath Numerical Renormalization Group Method and Successive Collective Screening in Multi-Impurity Kondo Systems

Danqing Hu,^{1,2} Jiangfan Wang,³ and Yi-feng Yang^{1,4,5,*}

¹*Beijing National Laboratory for Condensed Matter Physics and Institute of Physics, Chinese Academy of Sciences, Beijing 100190, China*

²*Department of Physics and Chongqing Key Laboratory for Strongly Coupled Physics, Chongqing University, Chongqing 401331, China*

³*School of Physics, Hangzhou Normal University, Hangzhou, Zhejiang 311121, China*

⁴*School of Physical Sciences, University of Chinese Academy of Sciences, Beijing 100049, China*

⁵*Songshan Lake Materials Laboratory, Dongguan, Guangdong 523808, China*

(Dated: May 18, 2023)

We propose an auxiliary-bath algorithm for the numerical renormalization group (NRG) method to solve multi-impurity models with shared electron baths. The method allows us to disentangle the electron baths into independent Wilson chains to perform standard NRG procedures beyond the widely adopted independent bath approximation. Its application to the 2-impurity model immediately reproduces the well-known even- and odd-parity channels. For 3-impurity Kondo models, we find successive screening of collective degrees of freedom such as the helicity and the cluster spin, and clarify the false prediction of a non-Fermi liquid ground state in unphysical parameter region in previous literature due to improper treatment of disentanglement. Our work highlights the importance of nonlocal spatial correlations due to shared baths and reveals a generic picture of successive collective screening for the entropy depletion that is crucial in real correlated systems. Our method greatly expands the applicability of the NRG and opens an avenue for its further development.

Quantum impurity models play an important role in modern condensed matter studies because of their fundamental importance for correlated electron physics and practical applications in mesoscopic systems [1–9]. As minimal interacting models, they contain the seeds of many exotic quantum many-body phenomena such as the local Fermi liquid [10–13], the non-Fermi liquid (NFL) with anyon excitations [14–19], or the competition between Kondo screening and the induced Rudermann-Kittel-Kasuya-Yosida (RKKY) interaction that underlies the basic physics of heavy fermion systems [20–24]. They have also been used to understand lattice problems and calculate material properties within the framework of dynamical mean-field theory [25–27].

Among all methods developed for solving the impurity models [28–33], Wilson’s numerical renormalization group (NRG) [28, 29] has been successfully applied to the single impurity Kondo problem and can in principle yield highly accurate results over wide energy and temperature ranges for very general impurity interactions, where quantum Monte Carlo methods often suffer from severe sign problem. However, its application to multi-impurity models has been severely limited by its own methodology, which requires to first map the electron baths to independent conduction (Wilson) chains coupled to the impurities [34–42]. This prerequisite is generally not possible except for very rare cases [43–49], because the impurities often couple to the shared electron baths in different momentum-dependent form that cannot be easily disentangled. Therefore, many works assume models with independent baths and artificial exchange interactions between impurities, based on which various ground

state phase diagrams have been predicted [34–42, 50], but real systems often have shared baths that not only cause the Kondo screening but also mediate the RKKY interaction. This hinders wider applications of NRG.

In this work, we propose a general strategy named the auxiliary-bath NRG to disentangle the shared baths into a minimal number of independent auxiliary baths coupled to the impurities in momentum-independent form and map them to Wilson chains following the standard NRG procedure. Our method naturally reproduces the effective odd- and even-parity channels for 2-impurity model [45]. Its application to the 3-impurity Kondo model reveals a minimal 4 auxiliary baths instead of 3 assumed in most literature. Under C_3 symmetry, our calculations yield a tentative phase diagram of successive screening of collective degrees of freedom such as helicity and cluster spin over a wide parameter region. We find no sign of NFL ground state and clarify the origin of the false prediction in previous work [47–49]. Our work highlights the importance of shared-bath models and collective screening in real systems, and opens an avenue for further development of the NRG.

We consider as an example the N -impurity model consisting of two parts, $H = H_I + H_B$, where H_I represents a general model of interacting impurities ($f_{\mu\sigma}$) and H_B describes their coupling to a free electron bath ($c_{\mathbf{k}\sigma}$):

$$H_B = \sum_{\mathbf{k}\sigma} \epsilon_{\mathbf{k}} c_{\mathbf{k}\sigma}^\dagger c_{\mathbf{k}\sigma} + \sum_{\mathbf{k}\mu\sigma} V_{\mathbf{k}\mu} (f_{\mu\sigma}^\dagger c_{\mathbf{k}\sigma} + \text{H.c.}) \quad (1)$$

where $V_{\mathbf{k}\mu} = V_\mu e^{i\mathbf{k}\cdot\mathbf{r}_\mu}$ with V_μ being the local hybridization strength of the μ -th ($\mu = 1, \dots, N$) impurity with the bath at the lattice site \mathbf{r}_μ . The shared-bath model is

generally unsolvable for traditional NRG algorithm because it is impossible to disentangle the bath and generate the Wilson chain for each impurity independently. This is easy to see because independent chains cannot induce the inter-impurity RKKY interaction.

To overcome this difficulty, we notice that as long as only the impurity degrees of freedom are considered, we may integrate out the conduction electrons and derive the effective action:

$$S_I^{\text{eff}} = S_I - \sum_{\mu\nu\sigma n} f_{\mu\sigma,n}^\dagger \mathcal{B}_{\mu\nu}(i\omega_n) f_{\nu\sigma,n}, \quad (2)$$

where S_I is the action of the impurities alone given by H_I , $\mathcal{B}_{\mu\nu}(i\omega_n) = \sum_{\mathbf{k}} \frac{V_{\mu\mathbf{k}} V_{\nu\mathbf{k}}^*}{i\omega_n - \epsilon_{\mathbf{k}}}$ is induced by their coupling to the shared bath, and the subscript n denotes the fermionic Matsubara frequency ω_n . Hence, solving the impurity model only requires correct $\mathcal{B}_{\mu\nu}(i\omega_n)$ regardless of its origin. This motivates us to introduce an effective model with auxiliary baths coupled \mathbf{k} -independently to all impurities:

$$H_{AU} = \sum_{\mathbf{k}p\sigma} E_{\mathbf{k}}^p \tilde{c}_{\mathbf{k}p\sigma}^\dagger \tilde{c}_{\mathbf{k}p\sigma} + \sum_{\mathbf{k}\mu p\sigma} (W_{\mu p} f_{\mu\sigma}^\dagger \tilde{c}_{\mathbf{k}p\sigma} + \text{H.c.}), \quad (3)$$

where $\tilde{c}_{\mathbf{k}p\sigma}$ ($p = 0, 1, \dots, N_A - 1$) denote the N_A auxiliary baths satisfying

$$\sum_{p\mathbf{k}} \frac{W_{\mu p} W_{\nu p}^*}{i\omega_n - E_{\mathbf{k}}^p} = \sum_{\mathbf{k}} \frac{V_{\mu\mathbf{k}} V_{\nu\mathbf{k}}^*}{i\omega_n - \epsilon_{\mathbf{k}}} = \mathcal{B}_{\mu\nu}(i\omega_n). \quad (4)$$

Replacing the sum over momentum by integration over energy, we derive the equations:

$$\sum_p w_{\mu p} w_{\nu p}^* \tilde{\rho}_p(\omega) = \rho_{\mu\nu}(\omega) \equiv \sum_{\mathbf{k}} e^{i\mathbf{k}\cdot(\mathbf{r}_\mu - \mathbf{r}_\nu)} \delta(\omega - \epsilon_{\mathbf{k}}), \quad (5)$$

where we have defined the dimensionless coupling parameters $w_{\mu p} = W_{\mu p}/V_\mu$, and $\tilde{\rho}_p(\omega)$ are the densities of states of the auxiliary baths to be solved and used in NRG. For $\mu = \nu$, we have $\rho_{\mu\mu}(\omega) = \rho_0(\omega) \equiv \sum_{\mathbf{k}} \delta(\omega - \epsilon_{\mathbf{k}})$, which is the density of states (DOS) of the original bath. Integrating over the energy leads to $\sum_p w_{\mu p} w_{\nu p}^* = \delta_{\mu\nu}$, which implies that $\{w_{\mu p}\}$ forms an $N \times N_A$ complex matrix whose row vectors $\mathbf{w}_\mu \equiv \{w_{\mu p}\}$ are orthonormalized. Physically, this follows from the mapping $c_{\mu\sigma} \rightarrow \sum_{\mathbf{k}p} w_{\mu p} \tilde{c}_{\mathbf{k}p\sigma} = \sum_p w_{\mu p} \tilde{c}_{p\sigma}$ and the commutation relation. The fact that each auxiliary bath couples to all impurities $f_{\mu\sigma}$ in a momentum-independent manner in H_{AU} allows the standard NRG procedure to transform it into an independent Wilson chain.

In general, $\rho_{\mu\nu}(\omega)$ for $\mu \neq \nu$ are complex so that $w_{\mu p}$ should also be complex. However, if $\epsilon_{\mathbf{k}} = \epsilon_{-\mathbf{k}}$, e.g., under spatial inversion or time reversal symmetry, we have $\text{Im}\rho_{\mu\nu}(\omega) = \sum_{\mathbf{k}} \sin[\mathbf{k}\cdot(\mathbf{r}_\mu - \mathbf{r}_\nu)] \delta(\omega - \epsilon_{\mathbf{k}}) = 0$, and $w_{\mu p}$ may take real values. Since $\rho_{\mu\nu} = \rho_{\nu\mu}^*$, the number of independent equations for $\tilde{\rho}_p(\omega)$ is reduced to

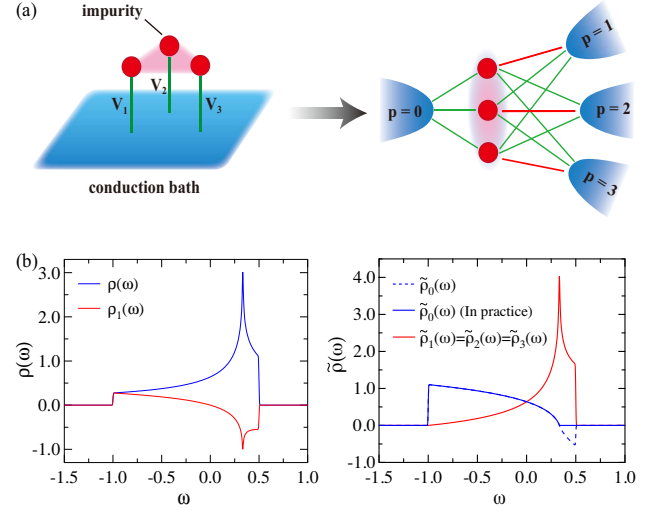


FIG. 1: (a) Illustration of the auxiliary-bath NRG that maps the original shared bath (left) to several auxiliary baths (right) where the green (red) lines indicate a positive (negative) sign of the dimensionless coupling parameter $w_{\mu p}$. (b) Comparison of the diagonal and off-diagonal densities of states of the original bath (left) and the auxiliary baths (right) for the C_3 symmetric 3-impurity model on a triangle lattice. The dashed line indicates negative $\tilde{\rho}_p(\omega)$ of the auxiliary baths, which is set to 0 in practice. The bandwidth of the original bath is set to $D = 1.5$ as the basic energy scale.

$N_A = \frac{N(N-1)}{2} + 1$, which is also the minimal number of auxiliary baths $\tilde{\rho}_p(\omega)$ to satisfy the constraint for the N -impurity model. All spatial information of the impurities is absorbed in the DOS of the auxiliary baths. For instance, the 2-impurity model requires $N_A = 2$ and Eq. (5) can be easily solved, giving $\tilde{\rho}_p(\omega) = \rho_0(\omega) \pm \rho_{12}(\omega)$ and $\mathbf{w}_\mu = \{1/\sqrt{2}, \pm 1/\sqrt{2}\}$, which are exactly the effective baths coupled to the odd- and even-parity combinations of local orbitals in previous work [45].

Obviously, the above procedure is independent of the impurity Hamiltonian H_I and the model symmetry. To show the advantage of our approach, we study as an example the symmetric 3-impurity model with a single shared bath on a triangle lattice, which is a minimal model for exploring the interplay between Kondo physics and magnetic frustrations and has not been thoroughly understood [47–49, 51–54]. Previous NRG calculations based on an effective 3-band model predicted an exotic NFL ground state with irrational degeneracy in some parameter region [47]. We find immediately a problem, namely the minimal number of auxiliary baths to reproduce the original model is $N_A = 4$ instead of 3 [55]. Under C_3 symmetry, we may further set $V_\mu = V$, the impurity distance $R_{12} = R_{13} = R_{23} = a$ (a is the lattice parameter), and $\rho_{\mu\nu}(\omega) = \rho_1(\omega)$ for $\mu \neq \nu$. As shown in the Supplemental Material [55], the coupling parameters are solved to be $|w_{\mu p}| = 1/2$ with their signs illustrated by different colors in Fig. 1(a), and the effective model

contains one auxiliary bath $\tilde{\rho}_0(\omega) = \rho_0(\omega) + 3\rho_1(\omega)$ coupled equally to all impurities and three other auxiliary baths ($p = 1, 2, 3$) of the same $\tilde{\rho}_p(\omega) = \rho_0(\omega) - \rho_1(\omega)$ coupled to impurities differently. One may notice in Fig. 1(b) that the latter has negative DOS in a narrow high energy region (dashed line), which has no significant influence on low energy physics and can be safely set to zero for approximation.

To compare with the literature [47], we take $H_I = U \sum_{\mu} (n_{\mu\uparrow} - \frac{1}{2})(n_{\mu\downarrow} - \frac{1}{2})$ and perform numerical calculations on the following effective spin model after projecting out the impurity charge degrees of freedom via the Schrieffer-Wolff (SW) transformation [55]:

$$H = \sum_{\mathbf{k}p\sigma} E_{\mathbf{k}}^p \tilde{c}_{\mathbf{k}p\sigma}^{\dagger} \tilde{c}_{\mathbf{k}p\sigma} + \sum_{pp'\mu} J_{\mu}^{pp'} \mathbf{S}_{\mu} \cdot \mathbf{s}_{pp'}, \quad (6)$$

in which $J_{\mu}^{pp'} = \frac{8V^2}{U} w_{\mu p}^* w_{\mu p'}$, $\mathbf{S}_{\mu} = \frac{1}{2} \sum_{\alpha\beta} f_{\mu\alpha}^{\dagger} \boldsymbol{\sigma}_{\alpha\beta} f_{\mu\beta}$, and $\mathbf{s}_{pp'} = \frac{1}{2} \sum_{\alpha\beta} \tilde{c}_{p\alpha}^{\dagger} \boldsymbol{\sigma}_{\alpha\beta} \tilde{c}_{p'\beta}$. Because the mapping operation commutes with the SW transformation, the above model can also be obtained by applying the mapping directly to the Kondo Hamiltonian using $\mathbf{s}_{\mu} \rightarrow \sum_{pp'} w_{\mu p}^* w_{\mu p'} \mathbf{s}_{pp'}$. This generates Kondo scattering between auxiliary baths, which is missing under independent bath assumption. One can prove that the RKKY interaction derived from Eq. (6) is identical to that from the original model [55]. The effective spin model is then solved by using the interleaving approach [56, 57]. We choose the NRG discretization parameter $\Lambda = 20$ to separate energy scales, and keep a fixed number of N_s states for each NRG step.

Figure 2(a) compares the calculated impurity entropy $S_{\text{imp}} = S - S_0$ for different N_s at $\alpha = \pi(V/D)^2 = 0.025$ for a fixed $U/D = 2$, where S is the total entropy of the impurity model and S_0 is that of the noninteracting model without impurities. We see clear steps at $2 \ln 2$ and $\ln 2$ despite of oscillations in some regions. As N_s increases, the oscillations diminish and their minima approach the steps as shown in Fig. 2(b), confirming the entropy plateaus at $2 \ln 2$ and $\ln 2$.

To understand the nature of these plateaus, we further calculate the spin-spin correlation $\langle \mathbf{S}_1 \cdot \mathbf{S}_2 \rangle$ and the effective total spin moment of the impurities, $\mu_{\text{eff}} = T\chi = \langle S_z^2 \rangle - \langle S_z \rangle_0$, where S_z is the z -component spin of the whole system and the subscript 0 refers to the noninteracting system without the impurities [58]. The results are plotted in Fig. 3 as functions of the temperature T for different values of α [59]. At high temperatures, the entropy always approaches $3 \ln 2$ and the effective moment $\mu_{\text{eff}} = 3/4$, indicating free local moments without spin-spin correlations. With lowering temperature, the entropy decreases. Accordingly, $\langle \mathbf{S}_1 \cdot \mathbf{S}_2 \rangle$ turns negative and its magnitude increases, marking the onset of antiferromagnetic correlations between impurities due to the RKKY interaction. For small α such as 0.025 and 0.06, the entropy first drops to $2 \ln 2$ as the spin-spin corre-

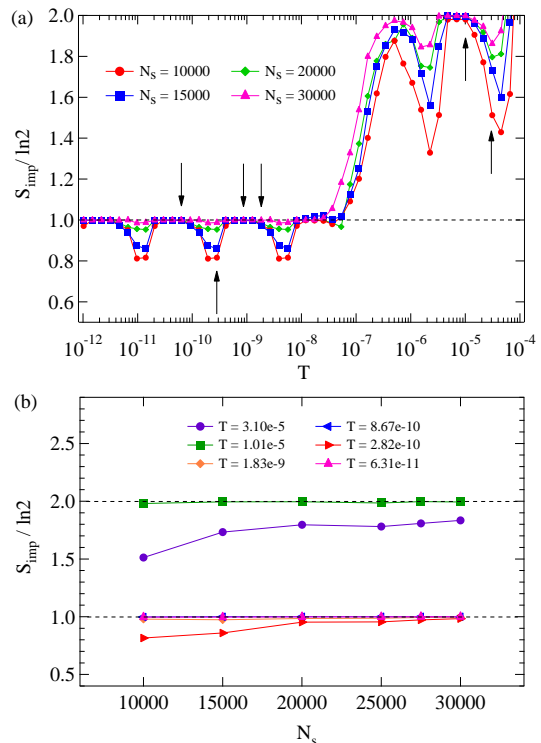


FIG. 2: (a) Typical impurity entropy S_{imp} as a function of the temperature T for different N_s of the kept states at $\alpha = 0.025$, showing plateaus at $2 \ln 2$, $\ln 2$ and oscillations in some regions that diminish with increasing N_s . (b) Convergence of S_{imp} to the plateau values with increasing N_s for the temperatures marked by arrows in (a).

lation $\langle \mathbf{S}_1 \cdot \mathbf{S}_2 \rangle$ approaches $-1/4$ and the effective moment μ_{eff} drops to $1/4$. This arises from the four-fold degenerate cluster impurity states characterized by the total spin $S_{\text{tot}} = 1/2$ and helicity $h = \pm 1$ [55]. The $S_{\text{tot}} = 3/2$ high spin quartet with $h = 0$ has a higher energy due to the antiferromagnetic RKKY interaction and are quenched in this temperature region. Further lowering the temperature, the entropy drops to $\ln 2$, but the spin-spin correlation and the effective moment remains unchanged, indicating that the cluster spin degree of freedom is not affected. Hence, this effect must be due to the quench of the helicity degree of freedom, which forms a pseudospin and couples with the auxiliary baths $\tilde{c}_{h\alpha} = \frac{1}{\sqrt{3}} \sum_{p=1}^3 e^{i2\pi h(p-1)/3} \tilde{c}_{p\alpha}$. It reflects the screening of nonlocal orbital motion of the multi-impurity system, which occurs prior to the screening of the cluster spin degree of freedom and causes the drop of the total impurity entropy from $2 \ln 2$ to $\ln 2$. For sufficiently small $\alpha = 0.025$, this state persists to the lowest temperature we have calculated. For a slightly larger $\alpha = 0.06$, both the entropy and μ_{eff} drop to zero at slightly lower temperature, indicating the Kondo screening of the remaining cluster spin degree of freedom. For even larger α ,

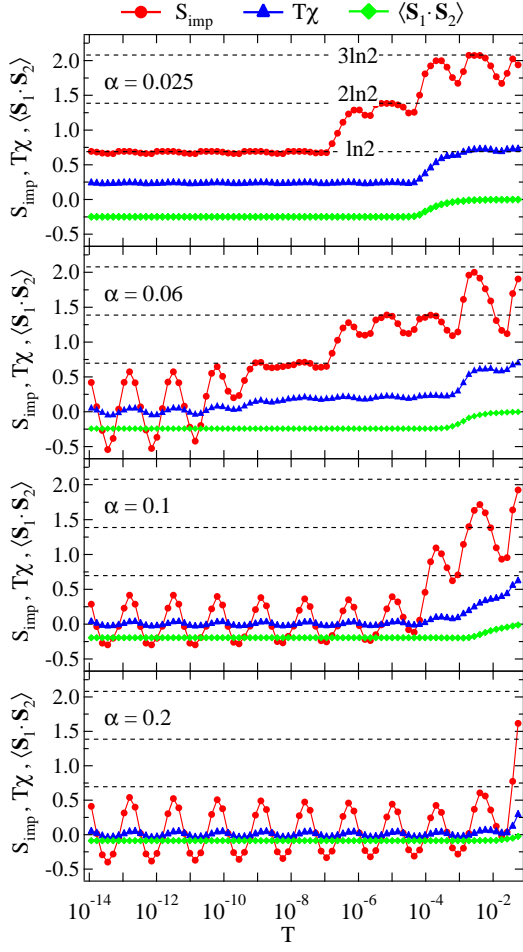


FIG. 3: Comparison of the impurity entropy S_{imp} , the effective spin moment $\mu_{\text{eff}} \equiv T\chi$, where χ is the impurity spin susceptibility, and the spin-spin correlation $\langle \mathbf{S}_1 \cdot \mathbf{S}_2 \rangle$ as functions of the temperature T for $\alpha = 0.025, 0.06, 0.1, 0.2$. The dashed lines mark the entropy plateaus at $3\ln 2$, $2\ln 2$, and $\ln 2$. To reduce computational time, all results are obtained for $N_s = 25000$.

the entropy drops directly from $3\ln 2$ to 0, below which μ_{eff} remains zero, implying that the spins are quickly screened due to the large Kondo coupling. Interestingly, the spin-spin correlation increases gradually from $-1/4$ to a small negative value, indicating the destruction of cluster spin degree of freedom so that the screening partly happens directly on individual impurity spins. The qualitative differences between small and large α reflect the crossover from collective screening of cluster degrees of freedom to the screening of individual impurities.

To have an overall picture, we map out a tentative $T-\alpha$ phase diagram in Fig. 4(b), where the phase crossover is roughly estimated by the entropy crossover between two plateaus. The phase diagram shows clear multi-step process for the entropy depletion. Depending on the value of α , it occurs successively with lowering temperature, from

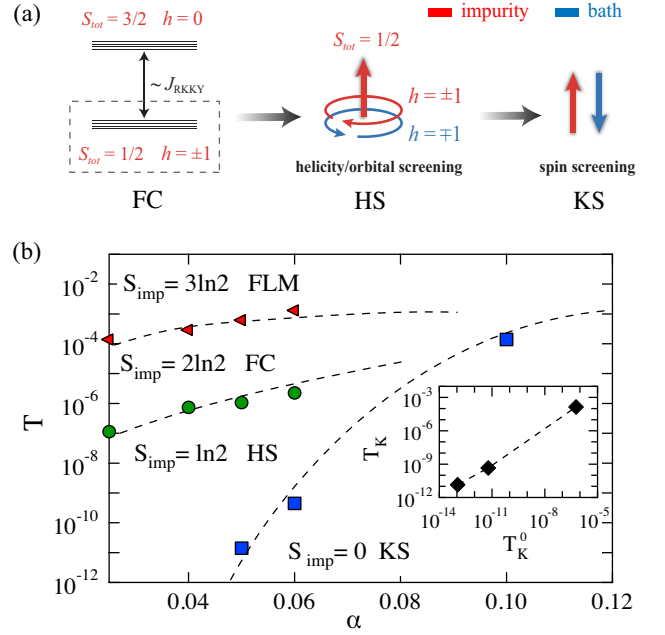


FIG. 4: (a) A schematic plot of the successive entropy depletion due to the frustrated cluster (FC) states, the helicity screening (HS), and the Kondo screening of the cluster spin degree of freedom (KS). (b) A tentative $T-\alpha$ phase diagram constructed based on the entropy crossover (half integer of $\ln 2$). The dashed lines are guides to the eye. The insert shows the much enhanced cluster spin screening temperature (T_K) and the single impurity Kondo temperature (T_K^0).

free local moments (FLM) with $S_{\text{imp}} = 3\ln 2$, $\mu_{\text{eff}} = 3/4$, $\langle \mathbf{S}_1 \cdot \mathbf{S}_2 \rangle = 0$, to a frustrated cluster (FC) state with $S_{\text{imp}} = 2\ln 2$, $\mu_{\text{eff}} = 1/4$, $\langle \mathbf{S}_1 \cdot \mathbf{S}_2 \rangle = -1/4$, to helicity screening (HS) with $S_{\text{imp}} = \ln 2$, $\mu_{\text{eff}} = 1/4$, $\langle \mathbf{S}_1 \cdot \mathbf{S}_2 \rangle = -1/4$, and eventually to a fully Kondo screened (KS) region with $S_{\text{imp}} = 0$, $\mu_{\text{eff}} = 0$, and $\langle \mathbf{S}_1 \cdot \mathbf{S}_2 \rangle$ varying from $-1/4$ to 0 as the cluster spin degree of freedom is destructed with increasing α . This overall picture is illustrated in Fig. 4(a), marking a typical physical process of the entropy depletion in multi-impurity systems, where the screening takes place successively on emergent collective degrees of freedom rather than individual original spins over a broad parameter region of moderate α . Interestingly, as shown in the inset of Fig. 4(b), the cluster spin screening temperature (T_K) is greatly enhanced compared to the single impurity Kondo temperature, T_K^0 , in this region.

Previous works based on 3-band assumption have predicted a NFL state with irrational degeneracy for the C_3 symmetric 3-impurity model [47–49, 53]. Our calculations show no sign of such an exotic state. To clarify the origin of this discrepancy, we ignore the $p = 0$ bath and rewrite our effective Hamiltonian in their proposed form. As shown in the Supplemental Material [55], the corresponding parameters are constrained and located in a region of independent Kondo screening in the phase

diagram proposed in Ref. [47]. We therefore conclude that their predicted frustrated NFL fixed point [47–49] is an artefact of their independent parameter assumption, which ignores falsely the parameter relations in the effective spin model and pushes the phase space into unphysical regions. It has been argued that the parameters may be tuned if the impurities are not on the lattice sites. We have examined this and found no change in the conclusion [55]. In Ref. [53], the same NFL fixed point was obtained by perturbative renormalization group calculations on a similar effective Hamiltonian as studied in Ref. [49], possibly due to incorrect treatment of disentanglement. It will be interesting to see if such an exotic fixed point might be realized in other circumstances.

Our method may be applied to general N -impurity models with arbitrary lattice or impurity geometries and hybridization strengths. It provides an unambiguous way to disentangle the conduction electron states into independent auxiliary baths with two important consequences: (1) It allows for inter-bath scattering that helps stabilize the Fermi liquid ground state; (2) It correctly produces the RKKY interaction to avoid artificial treatment of inter-impurity correlations. The mapping also gives naturally the auxiliary parameters without uncontrolled approximations. Numerical computations for larger N are time involving and require more efficient NRG algorithms, but our method can still be applied to disentangle the shared bath.

Our results have important implications on general Kondo models with shared baths. In the presence of symmetry, the impurity spins always tend to form some collective degrees of freedom to be successively screened with lowering temperature or other tuning parameters. Our phase diagram reveals additional temperature scales associated with the successive screening of these collective degrees of freedom to replace the screening of each impurity individually. One may expect that, as the number of impurities grows such as in a lattice, the number of effective collective degrees of freedom also increases, causing more and more entropy plateaus and eventually a continuous depletion of the magnetic entropy per spin observed in real materials. Therefore, the screening in multi-impurity or lattice Kondo systems with shared baths is generally nonlocal except for extremely large Kondo couplings. This reveals some fundamental aspects of the Kondo lattice physics [60–64], and suggests a generic picture beyond the oversimplified Doniach paradigm [23].

This work was supported by the National Natural Science Foundation of China (Grants No. 11974397 and No. 12174429), the National Key R&D Program of China (Grant No. 2022YFA1402203), and the Strategic Priority Research Program of the Chinese Academy of Sciences (Grant No. XDB33010100).

D.H. and J.W. contributed equally to this work.

* yifeng@iphy.ac.cn

- [1] S. Sasaki, S. De Franceschi, J. M. Elzerman, W. G. van der Wiel, M. Eto, S. Tarucha, and L. P. Kouwenhoven, Kondo effect in an integer-spin quantum dot, *Nature* **405**, 764 (2000).
- [2] T. Jamneala, V. Madhavan, and M. F. Crommie, Kondo response of a single antiferromagnetic chromium trimer, *Phys. Rev. Lett.* **87**, 256804 (2001).
- [3] J. Park, A. N. Pasupathy, J. I. Goldsmith, C. Chang, Y. Yaish, J. R. Petta, M. Rinkoski, J. P. Sethna, H. D. Abruña, P. L. McEuen, and D. C. Ralph, Coulomb blockade and the Kondo effect in single-atom transistors, *Nature* **417**, 722 (2002).
- [4] N. Knorr, M. A. Schneider, L. Diekhöner, P. Wahl, and K. Kern, Kondo Effect of Single Co Adatoms on Cu Surfaces, *Phys. Rev. Lett.* **88**, 096804 (2002).
- [5] M. Pustilnik and L. Glazman, Kondo effect in quantum dots, *J. Phys. Condens. Matter* **16**, R513 (2004).
- [6] J. Bork, Y. Zhang, L. Diekhöner, L. Borda, P. Simon, J. Kroha, P. Wahl, and K. Kern, A tunable two-impurity Kondo system in an atomic point contact, *Nat. Phys.* **7**, 901 (2011).
- [7] H. Prušer, P. E. Dargel, M. Bouhassoune, R. G. Ulbrich, T. Pruschke, S. Lounis and Martin Wenderoth, Interplay between the Kondo effect and the Ruderman-Kittel-Kasuya-Yosida interaction, *Nat. Commun.* **5**, 5417 (2014).
- [8] A. J. Keller, L. Peeters, C. P. Moca, I. Weymann, D. Mahalu, V. Umansky, G. Zaránd, and D. Goldhaber-Gordon, Universal Fermi liquid crossover and quantum criticality in a mesoscopic system, *Nature* **526**, 237 (2015).
- [9] Z. Iftikhar, A. Anthore, A. K. Mitchell, F. D. Parmentier, U. Gennser, A. Ouerghi, A. Cavanna, C. Mora, P. Simon, F. Pierre, Tunable quantum criticality and super-ballistic transport in a “charge” Kondo circuit, *Science* **360**, 1315 (2018).
- [10] P. W. Anderson, Localized magnetic states in metals, *Phys. Rev.* **124**, 41 (1961).
- [11] J. Kondo, Resistance minimum in dilute magnetic alloys, *Prog. Theor. Phys.* **32**, 37 (1964).
- [12] P. Nozières, A “Fermi-liquid” description of the Kondo problem at low temperatures, *J. Low Temp. Phys.* **17**, 31 (1974).
- [13] A. C. Hewson, *The Kondo problem to heavy fermions*, (Cambridge University Press, Cambridge, England, 1993).
- [14] A. M. Tselick, The thermodynamics of multichannel Kondo problem, *J. Phys. C: Solid State Phys.* **18**, 159 (1985).
- [15] H. B. Pang and D. L. Cox, Stability of the fixed point of the two-channel Kondo Hamiltonian, *Phys. Rev. B* **44**, 9454 (1991).
- [16] G. Zaránd and J. von Delft, Analytical calculation of the finite-size crossover spectrum of the anisotropic two-channel Kondo model, *Phys. Rev. B.* **61**, 6918 (2000).
- [17] S. Yotsuhashi and H. Maebashi, Crossover temperature from non-Fermi liquid to Fermi liquid behavior in two types of impurity Kondo model, *J. Phys. Soc. Jpn.* **71**, 1705 (2002).
- [18] P. L. S. Lopes, I. Affleck, and E. Sela, Anyons in mul-

- tichannel Kondo systems, Phys. Rev. B **101**, 085141 (2020).
- [19] M. Lotem, E. Sela, and M. Goldstein, Manipulating non-Abelian anyons in a chiral multichannel Kondo model, Phys. Rev. Lett. **129**, 227703 (2022).
- [20] M. A. Ruderman and C. Kittel, Indirect exchange coupling of nuclear magnetic moments by conduction electrons, Phys. Rev. **96**, 99 (1954).
- [21] T. Kasuya, A theory of metallic ferro- and antiferromagnetism on Zener's model, Prog. Theor. Phys. **16**, 45 (1956).
- [22] K. Yosida, Magnetic properties of Cu-Mn alloys, Phys. Rev. **106**, 893 (1957).
- [23] S. Doniach, The Kondo lattice and weak antiferromagnetism, Physica B+C **91**, 231 (1977).
- [24] P. Coleman, *Introduction to Many-Body Physics*, (Cambridge University Press, Cambridge, United Kingdom, 2015).
- [25] M. J. Rozenberg, G. Kotliar, X. Y. Zhang, Mott-Hubbard transition in infinite dimensions. II, Phys. Rev. B **49**, 10181 (1994).
- [26] A. Georges, G. Kotliar, W. Krauth, and M. J. Rozenberg, Dynamical mean-field theory of strongly correlated fermion systems and the limit of infinite dimensions, Rev. Mod. Phys. **68**, 13 (1996).
- [27] T. Maier, M. Jarrell, T. Pruschke, and M. H. Hettler, Quantum cluster theories, Rev. Mod. Phys. **77**, 1027 (2005).
- [28] K. G. Wilson, The renormalization group: Critical phenomena and the Kondo problem, Rev. Mod. Phys. **47**, 773 (1975).
- [29] R. Bulla, T. A. Costi, and T. Pruschke, Numerical renormalization group method for quantum impurity systems, Rev. Mod. Phys. **80**, 395 (2008).
- [30] H. Kajueter, *Interpolating perturbation scheme for correlated electron systems*, Ph.D. thesis, Rutgers University, 1996.
- [31] M. Caffarel, W. Krauth, Exact diagonalization approach to correlated fermions in infinite dimensions: Mott transition and superconductivity, Phys. Rev. Lett. **72**, 1545 (1994).
- [32] J. E. Hirsch, R. M. Fye, Monte Carlo method for magnetic impurities in metals, Phys. Rev. Lett. **56**, 2521 (1986).
- [33] E. Gull, A. J. Millis, A. I. Lichtenstein, A. N. Rubtsov, M. Troyer, and P. Werner, Continuous-time Monte Carlo methods for quantum impurity models, Rev. Mod. Phys. **83**, 349 (2011).
- [34] M. Ferrero, L. De Leo, P. Lecheminant, and M. Fabrizio, Strong correlations in a nutshell, J. Phys. Condens. Matter **19**, 433201(2007).
- [35] R. Žitko and J. Bonča, Fermi-liquid versus non-Fermi-liquid behavior in triple quantum dots, Phys. Rev. Lett. **98**, 047203 (2007).
- [36] R. Žitko, and J. Bonča, Numerical renormalization group study of two-channel three-impurity triangular clusters, Phys. Rev. B **77**, 245112 (2008).
- [37] A. K. Mitchell, D. E. Logan, and H. R. Krishnamurthy, Two-channel Kondo physics in odd impurity chains, Phys. Rev. B **84**, 035119 (2011).
- [38] E. Sela, A. K. Mitchell, and L. Fritz, Exact crossover Green function in the two-channel and two-impurity Kondo models, Phys. Rev. Lett. **106**, 147202 (2011).
- [39] J. Bork, Y.-H. Zhang, L. Diekhöner, L. Borda, P. Simon, J. Kroha, P. Wahl and K. Kern, A tunable two-impurity Kondo system in an atomic point contact, Nat. Phys. **7**, 901 (2011).
- [40] A. K. Mitchell, E. Sela, and D. E. Logan, Two-channel Kondo physics in two-impurity Kondo models, Phys. Rev. Lett. **108**, 086405 (2012).
- [41] A. K. Mitchell, T. F. Jarrold, M. R. Galpin, and D. E. Logan, Local moment formation and Kondo screening in impurity trimers, J. Phys. Chem. B **117**, 12777 (2013).
- [42] F. Eickhoff and F. B. Anders, Strongly correlated multi-impurity models: The crossover from a single-impurity problem to lattice models, Phys. Rev. B **102**, 205132 (2020).
- [43] B. A. Jones and C. M. Varma, Study of two magnetic impurities in a Fermi gas, Phys. Rev. Lett. **58**, 843 (1987).
- [44] B. A. Jones, C. M. Varma, and J. W. Wilkins, Low-temperature properties of the two-impurity Kondo hamiltonian, Phys. Rev. Lett. **61**, 125 (1988).
- [45] L. Zhu and J.-X. Zhu, Coherence scale of coupled Anderson impurities, Phys. Rev. B **83**, 195103 (2011).
- [46] A. K. Mitchell and R. Bulla, Validity of the local self-energy approximation: Application to coupled quantum impurities, Phys. Rev. B **92**, 155101 (2015).
- [47] B. C. Paul and K. Ingersent, Frustration-induced non-Fermi-liquid behavior in a three-impurity Kondo model, arXiv:cond-mat/9607190 (1996).
- [48] B. C. Paul, *A study of a three-impurity Kondo model*, Ph.D. thesis, University of Florida, 2000.
- [49] K. Ingersent, A. W. W. Ludwig, and I. Affleck, Kondo screening in a magnetically frustrated nanostructure: Exact results on a stable non-Fermi-liquid phase, Phys. Rev. Lett. **95**, 257204 (2005).
- [50] E. J. König, P. Coleman, and Y. Komijani, Frustrated Kondo impurity triangle: A simple model of deconfinement, Phys. Rev. B **104**, 115103 (2021).
- [51] Yu. B. Kudasov and V. M. Uzdin, Kondo state for a compact Cr trimer on a metallic surface, Phys. Rev. Lett. **89**, 276802 (2002).
- [52] V. V. Savkin, A. N. Rubtsov, M. I. Katsnelson, and A. I. Lichtenstein, Correlated adatom trimer on a metal surface: A continuous-time quantum Monte Carlo study, Phys. Rev. Lett. **94**, 026402 (2005).
- [53] B. Lazarovits, P. Simon, G. Zaránd, and L. Szunyogh, Exotic Kondo effect from magnetic trimers, Phys. Rev. Lett. **95**, 077202 (2005).
- [54] J. Wang and Y.-F. Yang, Spin current Kondo effect in frustrated Kondo systems, Sci. China-Phys. Mech. Astron. **65**, 227212 (2022).
- [55] See the Supplemental Material for more details on the derivation of the auxiliary baths, the SW transformation for Eq. (6), the RKKY interaction, and the comparison with previous work.
- [56] A. K. Mitchell, M. R. Galpin, S. Wilson-Fletcher, D. E. Logan, and R. Bulla, Generalized wilson chain for solving multichannel quantum impurity problems, Phys. Rev. B **89**, 121105(R) (2014).
- [57] K. M. Stadler, A. K. Mitchell, J. von Delft, and A. Weichselbaum, Interleaved numerical renormalization group as an efficient multiband impurity solver, Phys. Rev. B **93**, 235101 (2016).
- [58] R. Žitko and J. Bonča, Multiple-impurity Anderson model for quantum dots coupled in parallel, Phys. Rev. B **74**, 045312 (2006).
- [59] For simplicity, the g factor, the Bohr magneton μ_B , and

the Boltzmann's constant k_B are all set to unity.

- [60] Y.-F. Yang, Z. Fisk, H.-O. Lee, J. D. Thompson, and D. Pines, Scaling the Kondo lattice, *Nature* **454**, 611 (2008).
- [61] G. Lonzarich, D. Pines, and Y.-F. Yang, Toward a new microscopic framework for Kondo lattice materials, *Rep. Prog. Phys.* **80**, 024501 (2017).
- [62] J. Wang and Y.-F. Yang, Nonlocal Kondo effect and quantum critical phase in heavy-fermion metals, *Phys. Rev. B* **104**, 165120 (2021).
- [63] J. Wang and Y.-F. Yang, Z_2 metallic spin liquid on a frustrated Kondo lattice, *Phys. Rev. B* **106**, 115135 (2022).
- [64] Y.-F. Yang, An emerging global picture of heavy fermion physics. *J. Phys. Condens. Matter* **35**, 103002 (2023).

Auxiliary-Bath Numerical Renormalization Group Method and Successive Collective Screening in Multi-Impurity Kondo Systems

- Supplemental Material -

Danqing Hu,^{1,2} Jiangfan Wang,³ and Yi-feng Yang^{1,4,5,*}

¹*Beijing National Laboratory for Condensed Matter Physics and Institute of Physics, Chinese Academy of Sciences, Beijing 100190, China*

²*Department of Physics and Chongqing Key Laboratory for Strongly Coupled Physics, Chongqing University, Chongqing 401331, China*

³*School of Physics, Hangzhou Normal University, Hangzhou, Zhejiang 311121, China*

⁴*School of Physical Sciences, University of Chinese Academy of Sciences, Beijing 100049, China*

⁵*Songshan Lake Materials Laboratory, Dongguan, Guangdong 523808, China*

I. Derivation of the auxiliary baths for the 3-impurity model

For a general 3-impurity model with $\epsilon_{\mathbf{k}} = \epsilon_{-\mathbf{k}}$, our mapping requires a minimal number of $N_A = 4$ auxiliary baths with real dimensionless coupling parameters $w_{\mu p} = W_{\mu p}/V_\mu$, whose densities of states $\tilde{\rho}_p(\omega)$ satisfy

$$\sum_p w_{\mu p} w_{\nu p} \tilde{\rho}_p(\omega) = \rho_{\mu\nu}(\omega), \quad (\text{S1})$$

where $p = 0, \dots, 3$ and $\mu, \nu = 1, 2, 3$. To reduce the number of independent equations, we require the three equations for $\mu = \nu$ to be linearly dependent such that

$$w_{1p}^2 = w_{2p}^2 = w_{3p}^2 = w_p^2 \quad \rightarrow \quad w_{\mu p} = \eta_{\mu p} |w_p|, \quad (\text{S2})$$

where $\eta_{\mu p} = \pm 1$ and $|w_p| = |w_{\mu p}|$. We then introduce a new label $l = 0, 1, 2, 3$ to denote the combined indices $(\mu, \nu) = (1, 1), (1, 2), (1, 3), (2, 3)$, so that Eq. (S1) may be rewritten as

$$\sum_p \mathcal{T}_{lp} |w_p|^2 \tilde{\rho}_p(\omega) = \rho_l(\omega) \quad (\text{S3})$$

with the coefficient matrix

$$\mathcal{T} = \begin{pmatrix} 1 & 1 & 1 & 1 \\ \eta_{10}\eta_{20} & \eta_{11}\eta_{21} & \eta_{12}\eta_{22} & \eta_{13}\eta_{23} \\ \eta_{10}\eta_{30} & \eta_{11}\eta_{31} & \eta_{12}\eta_{32} & \eta_{13}\eta_{33} \\ \eta_{20}\eta_{30} & \eta_{21}\eta_{31} & \eta_{22}\eta_{32} & \eta_{23}\eta_{33} \end{pmatrix}. \quad (\text{S4})$$

The linear equation (S3) can be inverted if and only if $\det \mathcal{T} \neq 0$. This leads to

$$\eta = \begin{pmatrix} 1 & -1 & 1 & 1 \\ 1 & 1 & -1 & 1 \\ 1 & 1 & 1 & -1 \end{pmatrix}, \quad (\text{S5})$$

which is unique up to arbitrary permutations between the p indices, and gives the signs of $w_{\mu p}$ illustrated in Fig. 1(a) of the main text. Equation (S3) then yields

$$\tilde{\rho}_p(\omega) = |w_p|^{-2} \sum_l [\mathcal{T}^{-1}]_{pl} \rho_l(\omega), \quad (\text{S6})$$

where

$$\mathcal{T}^{-1} = \frac{1}{4} \begin{pmatrix} 1 & 1 & 1 & 1 \\ 1 & -1 & -1 & 1 \\ 1 & -1 & 1 & -1 \\ 1 & 1 & -1 & -1 \end{pmatrix}. \quad (\text{S7})$$

The amplitudes $|w_p|$ can be determined by the normalization conditions for $\tilde{\rho}_p(\omega)$. Using $\int d\omega \rho_{\mu\nu}(\omega) = \delta_{\mu\nu}$ for onsite impurities, we obtain immediately $|w_p| = 1/2$. For the special C_3 symmetric case where $\rho_0(\omega) \neq \rho_1(\omega) = \rho_2(\omega) = \rho_3(\omega)$, the DOS of the auxiliary baths is $\tilde{\rho}_0(\omega) = \rho_0(\omega) + 3\rho_1(\omega)$ and $\tilde{\rho}_p(\omega) = \rho_0(\omega) - \rho_1(\omega)$ for $p = 1, 2, 3$, respectively, as given in the main text.

II. Proof of the least number of auxiliary baths for the 3-impurity model

We prove in a straightforward way here that the least number of auxiliary baths for the C_3 symmetric 3-impurity model is $N_A = 4$. We first notice that for $N = 3$, Eq. (S1) always contains 6 equations for any choice of N_A , including three diagonal ones ($\mu = \nu$) and three off-diagonal ones ($\mu \neq \nu$). In order for N_A baths to satisfy six equations, at least $6 - N_A$ equations should be linear combinations of the remaining N_A independent equations.

For $N_A = 2$, the only possibility is that one diagonal equation and one off-diagonal equation together determine the two auxiliary baths:

$$\begin{aligned} w_{11}^2 \tilde{\rho}_1(\omega) + w_{12}^2 \tilde{\rho}_2(\omega) &= \rho_0(\omega), \\ w_{11} w_{21} \tilde{\rho}_1(\omega) + w_{12} w_{22} \tilde{\rho}_2(\omega) &= \rho_1(\omega). \end{aligned} \quad (\text{S8})$$

The linear dependencies of the rest four equations on these two equations lead to the conditions in Eq. (S2) and

$$w_{1p} w_{2p} = w_{1p} w_{3p} = w_{2p} w_{3p} \quad (\text{S9})$$

for $p = 1, 2$. This gives the only solution, $\omega_{1p} = \omega_{2p} = \omega_{3p} = \pm |w_p|$, which violates the requirement of orthonormality. The coefficient matrix of Eq. (S8) becomes

$$\begin{pmatrix} |w_1|^2 & |w_2|^2 \\ |w_1|^2 & |w_2|^2 \end{pmatrix} = \begin{pmatrix} 1 & 1 \\ 1 & 1 \end{pmatrix}, \quad (\text{S10})$$

which cannot be inverted to give a solution of the two auxiliary baths.

For $N_A = 3$, one may choose either one diagonal and two off-diagonal equations, or one off-diagonal and two diagonal equations. For the first case, the three independent equations are

$$\begin{aligned} \sum_{p=1}^3 w_{1p}^2 \tilde{\rho}_p(\omega) &= \rho_0(\omega), \\ \sum_{p=1}^3 w_{1p} w_{2p} \tilde{\rho}_p(\omega) &= \rho_1(\omega), \\ \sum_{p=1}^3 w_{1p} w_{3p} \tilde{\rho}_p(\omega) &= \rho_1(\omega). \end{aligned} \quad (\text{S11})$$

Again, the linear dependencies of the other three equations give the conditions in Eq. (S2) and

$$\alpha w_{1p} w_{2p} + (1 - \alpha) w_{1p} w_{3p} = w_{2p} w_{3p}, \quad (\text{S12})$$

where α is an arbitrary real number. Equation (S11) can then be rewritten in the form of Eq. (S3) with the coefficient matrix:

$$\mathcal{T} = \begin{pmatrix} 1 & 1 & 1 \\ \eta_{11} \eta_{21} & \eta_{12} \eta_{22} & \eta_{13} \eta_{23} \\ \eta_{11} \eta_{31} & \eta_{12} \eta_{32} & \eta_{13} \eta_{33} \end{pmatrix}. \quad (\text{S13})$$

The column vector $\mathbf{A}_p = (\eta_{1p} \eta_{2p}, \eta_{1p} \eta_{3p})^T$ cannot be $(-1, -1)^T$, which is inconsistent with Eq. (S12). In addition, because $\mathbf{A}_p = (1, -1)^T$ and $(-1, 1)^T$ require different values of α , they cannot exist simultaneously in the coefficient matrix. As a result, \mathcal{T} contains at least two identical columns and is not invertible.

For the second case, we have the following three independent equations:

$$\begin{aligned} \sum_{p=1}^3 w_{1p}^2 \tilde{\rho}_p(\omega) &= \rho_0(\omega), \\ \sum_{p=1}^3 w_{2p}^2 \tilde{\rho}_p(\omega) &= \rho_0(\omega), \\ \sum_{p=1}^3 w_{1p} w_{2p} \tilde{\rho}_p(\omega) &= \rho_1(\omega). \end{aligned} \quad (\text{S14})$$

The linear dependencies of the other three equations give the conditions in Eq. (S9) and

$$\alpha w_{1p}^2 + (1 - \alpha)w_{2p}^2 = w_{3p}^2. \quad (\text{S15})$$

Eq. (S9) requires either $w_{1p} = w_{2p} = w_{3p} \neq 0$, which satisfies Eq. (S15) automatically for any α , or two of the three couplings (w_{1p}, w_{2p}, w_{3p}) being zero. Obviously, $w_{1p} = w_{2p} = 0, w_{3p} \neq 0$ is not a solution of Eq. (S15), while $w_{1p} = w_{3p} = 0, w_{2p} \neq 0$ and $w_{2p} = w_{3p} = 0, w_{1p} \neq 0$ requires different values of α to satisfy Eq. (S15) and are hence not allowed to appear simultaneously in the coefficient matrix:

$$\mathcal{T} = \begin{pmatrix} w_{11}^2 & w_{12}^2 & w_{13}^2 \\ w_{21}^2 & w_{22}^2 & w_{23}^2 \\ w_{11}w_{21} & w_{12}w_{22} & w_{13}w_{23} \end{pmatrix}. \quad (\text{S16})$$

Again, \mathcal{T} has at least two identical columns and does not have an inverse.

Taken together, $N_A = 2$ or 3 auxiliary baths are not enough to describe the C_3 symmetric 3-impurity model. The same conclusion should hold for general 3-impurity models since they typically cannot have less independent equations. Since $N_A = 4$ has been applied in previous section, we conclude that the least number of auxiliary baths is $N_A = 4$ for 3-impurity models.

III. The Schrieffer-Wolff transformation and the mapping of the Kondo models

In this section, we derive the Hamiltonian Eq. (6) in the main text using the Schrieffer-Wolff (SW) transformation. This is to suppress the charge degrees of freedom on the impurities to save the computation time. We start from the following 3-impurity Anderson model coupled to four leads:

$$H = \epsilon_0 \sum_{\mu\sigma} f_{\mu\sigma}^\dagger f_{\mu\sigma} + U \sum_{\mu} n_{\mu\uparrow}^f n_{\mu\downarrow}^f + \sum_{\mathbf{k}p\sigma} E_{\mathbf{k}}^p \tilde{c}_{\mathbf{k}p\sigma}^\dagger \tilde{c}_{\mathbf{k}p\sigma} + \sum_{\mathbf{k}\mu p\sigma} (W_{\mu p} f_{\mu\sigma}^\dagger \tilde{c}_{\mathbf{k}p\sigma} + \text{H.c.}), \quad (\text{S17})$$

where $W_{\mu p} = w_{\mu p}V = \eta_{\mu p}V/2$ are the new hybridization parameters. To perform the SW transformation, we first divide the Hilbert space into low energy (L) and high energy (H) subspaces. Because of the large onsite repulsion U , the atomic ground state corresponds to three f -electrons each occupying an impurity site, which we denote as f^3 . Their hybridizations with the baths result in high energy configurations like f^2, f^4, f^5 , etc. Here for simplicity, we will only consider the configurations with exactly one empty or doubly-occupied site (f^2 and f^4), which will be ‘‘integrated out’’ by the SW transformation. Other configurations are of higher energy and give higher order corrections. The resulting effective Hamiltonian contains a Kondo interaction term ΔH due to two types of virtual charge fluctuations. The one between f^3 and f^4 leads to

$$\Delta H_{(f^3+e^- \leftrightarrow f^4)} = - \sum_{pp'\alpha\beta\mu} W_{\mu p}^* W_{\mu p'} \frac{\tilde{c}_{p\alpha}^\dagger f_{\mu\alpha} f_{\mu\beta}^\dagger \tilde{c}_{p'\beta}}{\epsilon_0 + U}, \quad (\text{S18})$$

where $\tilde{c}_{p\beta} = \sum_{\mathbf{k}} \tilde{c}_{\mathbf{k}p\beta}$, and $\epsilon_0 + U$ is the energy difference between the configurations f^4 and f^3 . Rearranging the fermion operators gives $-\tilde{c}_{p\alpha}^\dagger \boldsymbol{\sigma}_{\alpha\beta} \tilde{c}_{p'\beta} \cdot \mathbf{S}_\mu$, plus an unimportant potential scattering term. Similarly, the fluctuation between f^3 and f^2 contributes

$$\Delta H_{(f^3 \leftrightarrow f^2+e^-)} = - \sum_{pp'\alpha\beta\mu} W_{\mu p}^* W_{\mu p'} \frac{f_{\mu\beta}^\dagger \tilde{c}_{p'\beta} \tilde{c}_{p\alpha}^\dagger f_{\mu\alpha}}{-\epsilon_0}. \quad (\text{S19})$$

Combining Eq. (S18) and Eq. (S19) gives

$$\Delta H = \sum_{pp'\alpha\beta\mu} W_{\mu p}^* W_{\mu p'} \left(\frac{1}{\epsilon_0 + U} - \frac{1}{\epsilon_0} \right) \tilde{c}_{p\alpha}^\dagger \boldsymbol{\sigma}_{\alpha\beta} \tilde{c}_{p'\beta} \cdot \mathbf{S}_\mu = \sum_{pp'\mu} J_\mu^{pp'} \mathbf{s}_{pp'} \cdot \mathbf{S}_\mu, \quad (\text{S20})$$

where $\mathbf{S}_\mu = \frac{1}{2} \sum_{\alpha\beta} f_{\mu\alpha}^\dagger \boldsymbol{\sigma}_{\alpha\beta} f_{\mu\beta}$, and $\mathbf{s}_{pp'} = \frac{1}{2} \sum_{\alpha\beta} \tilde{c}_{p\alpha}^\dagger \boldsymbol{\sigma}_{\alpha\beta} \tilde{c}_{p'\beta}$. For the particle-hole symmetric case ($\epsilon_0 = -U/2$), $J_\mu^{pp'} = \frac{8V^2}{U} w_{\mu p}^* w_{\mu p'} = J_K w_{\mu p}^* w_{\mu p'}$, which is exactly the results in the main text.

The above derivation gives a relation between the effective Kondo couplings and the hybridization parameters with auxiliary baths. In principle, the SW transformation and the mapping operation commute, so we may also apply the mapping directly to the Kondo Hamiltonian, $J_K \sum_{\mu} \mathbf{s}_\mu \cdot \mathbf{S}_\mu$, by using $c_{\mu\sigma} \rightarrow \sum_p w_{\mu p} \tilde{c}_{p\sigma}$ such that $\mathbf{s}_\mu \rightarrow \sum_{pp'} w_{\mu p}^* w_{\mu p'} \mathbf{s}_{pp'}$, although our mapping is derived from a hybridization model. We see from Eq. (S20) that the results are the same.

IV. Derivation of the RKKY interaction

The RKKY interaction of our auxiliary model Eq. (S20) can be derived similarly using the second-order perturbative calculations, giving

$$\begin{aligned}
H_{\text{RKKY}} &= \frac{1}{2} \sum_{\mu\mu'} J_{\text{RKKY}}(|\mathbf{r}_\mu - \mathbf{r}_{\mu'}|) \mathbf{S}_\mu \cdot \mathbf{S}_{\mu'}, \\
J_{\text{RKKY}}(|\mathbf{r}_\mu - \mathbf{r}_{\mu'}|) &= \frac{1}{2} \sum_{pp'} J_\mu^{pp'} J_{\mu'}^{p'p} \sum_{\mathbf{q}\mathbf{q}'} \frac{n_F(E_{\mathbf{q}}^p) - n_F(E_{\mathbf{q}'}^{p'})}{E_{\mathbf{q}}^p - E_{\mathbf{q}'}^{p'}},
\end{aligned} \tag{S21}$$

where n_F is the Fermi distribution function. The momentum sums can be replaced by the following energy integrals over the DOS of the auxiliary baths:

$$\sum_{\mathbf{q}\mathbf{q}'} \frac{n_F(E_{\mathbf{q}}^p) - n_F(E_{\mathbf{q}'}^{p'})}{E_{\mathbf{q}}^p - E_{\mathbf{q}'}^{p'}} = \int d\epsilon d\epsilon' \tilde{\rho}_p(\epsilon) \tilde{\rho}_{p'}(\epsilon') \frac{n_F(\epsilon) - n_F(\epsilon')}{\epsilon - \epsilon'}. \tag{S22}$$

Substituting $J_\mu^{pp'} = J_K w_{\mu p}^* w_{\mu p'}$ and Eq. (S22) into Eq. (S21), we have

$$\begin{aligned}
J_{\text{RKKY}}(|\mathbf{r}_\mu - \mathbf{r}_{\mu'}|) &= \frac{J_K^2}{2} \int d\epsilon d\epsilon' \left(\sum_p w_{\mu' p} w_{\mu p}^* \tilde{\rho}_p(\epsilon) \right) \left(\sum_{p'} w_{\mu p'} w_{\mu' p'}^* \tilde{\rho}_{p'}(\epsilon') \right) \frac{n_F(\epsilon) - n_F(\epsilon')}{\epsilon - \epsilon'} \\
&= \frac{J_K^2}{2} \int d\epsilon d\epsilon' \sum_{\mathbf{k}\mathbf{k}'} e^{i(\mathbf{k}-\mathbf{k}') \cdot (\mathbf{r}_{\mu'} - \mathbf{r}_\mu)} \delta(\epsilon - \epsilon_{\mathbf{k}}) \delta(\epsilon' - \epsilon_{\mathbf{k}'}) \frac{n_F(\epsilon) - n_F(\epsilon')}{\epsilon - \epsilon'} \\
&= \frac{J_K^2}{2} \sum_{\mathbf{k}\mathbf{k}'} e^{i(\mathbf{k}-\mathbf{k}') \cdot (\mathbf{r}_{\mu'} - \mathbf{r}_\mu)} \frac{n_F(\epsilon_{\mathbf{k}}) - n_F(\epsilon_{\mathbf{k}'})}{\epsilon_{\mathbf{k}} - \epsilon_{\mathbf{k}'}} \\
&= - \left(\frac{J_K}{2} \right)^2 \sum_{\mathbf{q}} e^{i\mathbf{q} \cdot (\mathbf{r}_\mu - \mathbf{r}_{\mu'})} \chi(\mathbf{q}),
\end{aligned} \tag{S23}$$

where

$$\chi(\mathbf{q}) = 2 \sum_{\mathbf{k}} \frac{n_F(\epsilon_{\mathbf{k}}) - n_F(\epsilon_{\mathbf{k}+\mathbf{q}})}{\epsilon_{\mathbf{k}+\mathbf{q}} - \epsilon_{\mathbf{k}}} \tag{S24}$$

is the susceptibility of the original conduction electron bath. Note that we have used Eq. (5) in the main text during the derivation, namely

$$\sum_p w_{\mu' p} w_{\mu p}^* \tilde{\rho}_p(\epsilon) = \rho_{\mu' \mu}(\epsilon) = \sum_{\mathbf{k}} e^{i\mathbf{k} \cdot (\mathbf{r}_{\mu'} - \mathbf{r}_\mu)} \delta(\epsilon - \epsilon_{\mathbf{k}}). \tag{S25}$$

Equation (S23) is exactly the usual expression derived directly from the Kondo lattice model [1]. We have thus proved that our mapping can correctly reproduce the RKKY interaction between impurities without artificial assumptions.

V. Cluster states of three interacting impurities

The local Hilbert space for the three impurities with C_3 symmetry and antiferromagnetic RKKY interactions can be constructed using the following Heisenberg Hamiltonian:

$$\begin{aligned}
H_{\text{imp}} &= J(\mathbf{S}_1 \cdot \mathbf{S}_2 + \mathbf{S}_1 \cdot \mathbf{S}_3 + \mathbf{S}_2 \cdot \mathbf{S}_3) \\
&= \frac{J}{2} [(\mathbf{S}_1 + \mathbf{S}_2 + \mathbf{S}_3)^2 - \mathbf{S}_1^2 - \mathbf{S}_2^2 - \mathbf{S}_3^2] \\
&= \frac{J}{2} [S_{\text{tot}}(S_{\text{tot}} + 1) - 3S(S + 1)].
\end{aligned} \tag{S26}$$

For $S = 1/2$, the total spin quantum number can be $S_{\text{tot}} = 1/2$ or $3/2$, giving $\langle \mathbf{S}_1 \cdot \mathbf{S}_2 \rangle = \langle H_{\text{imp}} \rangle / 3J = -1/4$ or $1/4$, respectively. The eigenstates of H_{imp} , labeled by $|S_{\text{tot}}, S_{\text{tot}}^z, h\rangle$, can be written in terms of the basis $|S_1^z S_2^z S_3^z\rangle$ as:

$$\begin{aligned}
\left| \frac{3}{2}, \frac{3}{2}, 0 \right\rangle &= |\uparrow\uparrow\uparrow\rangle \\
\left| \frac{3}{2}, \frac{1}{2}, 0 \right\rangle &= \frac{1}{\sqrt{3}}(|\downarrow\uparrow\uparrow\rangle + |\uparrow\downarrow\uparrow\rangle + |\uparrow\uparrow\downarrow\rangle) \\
\left| \frac{3}{2}, \frac{-1}{2}, 0 \right\rangle &= \frac{1}{\sqrt{3}}(|\uparrow\downarrow\downarrow\rangle + |\downarrow\uparrow\downarrow\rangle + |\downarrow\downarrow\uparrow\rangle) \\
\left| \frac{3}{2}, \frac{-3}{2}, 0 \right\rangle &= |\downarrow\downarrow\downarrow\rangle \\
\left| \frac{1}{2}, \frac{1}{2}, 1 \right\rangle &= \frac{1}{\sqrt{3}}(|\downarrow\uparrow\uparrow\rangle + e^{-i2\pi/3} |\uparrow\downarrow\uparrow\rangle + e^{i2\pi/3} |\uparrow\uparrow\downarrow\rangle) \\
\left| \frac{1}{2}, \frac{-1}{2}, 1 \right\rangle &= \frac{1}{\sqrt{3}}(|\uparrow\downarrow\downarrow\rangle + e^{-i2\pi/3} |\downarrow\uparrow\downarrow\rangle + e^{i2\pi/3} |\downarrow\downarrow\uparrow\rangle) \\
\left| \frac{1}{2}, \frac{1}{2}, -1 \right\rangle &= \frac{1}{\sqrt{3}}(|\downarrow\uparrow\uparrow\rangle + e^{i2\pi/3} |\uparrow\downarrow\uparrow\rangle + e^{-i2\pi/3} |\uparrow\uparrow\downarrow\rangle) \\
\left| \frac{1}{2}, \frac{-1}{2}, -1 \right\rangle &= \frac{1}{\sqrt{3}}(|\uparrow\downarrow\downarrow\rangle + e^{i2\pi/3} |\downarrow\uparrow\downarrow\rangle + e^{-i2\pi/3} |\downarrow\downarrow\uparrow\rangle),
\end{aligned} \tag{S27}$$

where \uparrow and \downarrow denote the up and down spin states. One can see that the state with helicity h obtains a phase factor $e^{i2\pi h/3}$ upon the C_3 transformation. For $J > 0$, the $S_{\text{tot}} = 1/2$, $h = \pm 1$ states form a ground state manifold with the energy $E_0 = -3J/4$, and the high spin quartet with $S_{\text{tot}} = 3/2$ and $h = 0$ are the excited states with the energy $E_1 = 3J/4$.

VI. Comparison with previous work

In previous work [2–4], the C_3 symmetric impurities were suggested to couple to three orthogonal conduction bands ($c_{h\alpha}$) with different helicities $h = 0, \pm 1$, and all parameters are assumed to be independent, giving

$$\begin{aligned}
H_{\text{int}} &= [J_{00}\mathbf{s}_{00} + J_{11}(\mathbf{s}_{11} + \mathbf{s}_{\bar{1}\bar{1}})] \cdot \mathbf{S}_0 + [J_{01}(\mathbf{s}_{01} + \mathbf{s}_{\bar{1}0}) + J_{1\bar{1}}\mathbf{s}_{1\bar{1}}] \cdot \mathbf{S}_1 \\
&\quad + [J_{01}(\mathbf{s}_{10} + \mathbf{s}_{0\bar{1}}) + J_{\bar{1}\bar{1}}\mathbf{s}_{\bar{1}\bar{1}}] \cdot \mathbf{S}_{\bar{1}},
\end{aligned} \tag{S28}$$

where $\bar{1} \equiv -1$, $\mathbf{S}_h = \sum_{\mu} e^{-i2\pi(\mu-1)h/3} \mathbf{S}_{\mu}$, and $\mathbf{s}_{hh'} = \frac{1}{2} \sum_{\alpha\beta} c_{h\alpha}^{\dagger} \boldsymbol{\sigma}_{\alpha\beta} c_{h'\beta}$. The independent parameters were believed to capture arbitrary impurity separations R [3]. To compare with their results, we extend here our calculations to non-integer R , in which case the impurities are located off the lattice sites and the frequency integrals of $\rho_{\mu\nu}(\omega)$ become

$$\int d\omega \rho_{\mu\mu}(\omega) = \int d\omega \sum_{\mathbf{k}} \delta(\omega - \epsilon_{\mathbf{k}}) = 1, \tag{S29}$$

and, for $\mu \neq \nu$,

$$\begin{aligned}
\int d\omega \rho_{\mu\nu}(\omega) &= \int d\omega \sum_{\mathbf{k}} e^{i\mathbf{k} \cdot (\mathbf{r}_{\mu} - \mathbf{r}_{\nu})} \delta(\omega - \epsilon_{\mathbf{k}}) = \frac{1}{V_{\text{B.Z.}}} \int_{\text{B.Z.}} d^2\mathbf{k} \cos(k_x R) \\
&= \frac{3}{2\pi^2 R^2} \left(\cos \frac{2\pi R}{3} - \cos \frac{4\pi R}{3} \right),
\end{aligned} \tag{S30}$$

where we have used the C_3 symmetry and the Brillouin zone volume $V_{\text{B.Z.}} = 2\pi^2/\sqrt{3}$ for the triangle lattice. Combining these with Eq. (S6), we obtain

$$|w_p| = \begin{cases} \frac{1}{2} \sqrt{1 + \frac{9}{2\pi^2 R^2} \left(\cos \frac{2\pi R}{3} - \cos \frac{4\pi R}{3} \right)}, & p = 0 \\ \frac{1}{2} \sqrt{1 - \frac{3}{2\pi^2 R^2} \left(\cos \frac{2\pi R}{3} - \cos \frac{4\pi R}{3} \right)}, & p = 1, 2, 3 \end{cases} \tag{S31}$$

For integer R where the impurities are located on the lattice sites, the above results reduce to $|w_p| = 1/2$. For general R , the Kondo coupling in Eq. (S20) depends on R via

$$J_\mu^{pp'} = \frac{8V^2}{U} |w_p| |w_{p'}| \eta_{\mu p} \eta_{\mu p'}. \quad (\text{S32})$$

By dropping the $p = 0$ auxiliary bath and applying the same definition of \mathbf{S}_h and $\tilde{\mathbf{s}}_{hh'} = \frac{1}{2} \sum_{\alpha\beta} \tilde{c}_{h\alpha}^\dagger \boldsymbol{\sigma}_{\alpha\beta} \tilde{c}_{h'\beta}$ with $\tilde{c}_{h\sigma} = \frac{1}{\sqrt{3}} \sum_{p=1}^3 \tilde{c}_{p\sigma} e^{i2\pi h(p-1)/3}$, one can rewrite Eq. (S20) as:

$$\begin{aligned} \tilde{H}_{\text{int}} = & 4|w_1|^2 \{ [J_0 \tilde{\mathbf{s}}_{00} + 4J_0(\tilde{\mathbf{s}}_{11} + \tilde{\mathbf{s}}_{\bar{1}\bar{1}})] \cdot \mathbf{S}_0 + [-2J_0(\tilde{\mathbf{s}}_{01} + \tilde{\mathbf{s}}_{\bar{1}0}) + 4J_0 \tilde{\mathbf{s}}_{\bar{1}\bar{1}}] \cdot \mathbf{S}_1 \\ & + [-2J_0(\tilde{\mathbf{s}}_{10} + \tilde{\mathbf{s}}_{0\bar{1}}) + 4J_0 \tilde{\mathbf{s}}_{\bar{1}\bar{1}}] \cdot \mathbf{S}_{\bar{1}} \}, \end{aligned} \quad (\text{S33})$$

where $J_0 = \frac{2V^2}{3U}$. Comparing Eq. (S28) and Eq. (S33) leads to the requirement: $J_{11} = J_{\bar{1}\bar{1}} = 4J_{00}$ and $J_{01} = -2J_{00}$. As a result, the two parameters defined in previous work [2] to characterize their ground state phase diagram are, $K = (J_{00}^2 + 2J_{11}^2 - J_{\bar{1}\bar{1}}^2 - 2J_{01}^2)/(J_{00}^2 + 2J_{11}^2 + 2J_{\bar{1}\bar{1}}^2 + 4J_{01}^2) = 1/9$ and $\alpha = (J_{01} - J_{\bar{1}\bar{1}})/(J_{01} + J_{\bar{1}\bar{1}}) = -3$, which is located in the independent Kondo region. The claimed frustrated non-Fermi liquid fixed point is an unphysical artefact of their independent parameter approximation.

* yifeng@iphy.ac.cn

- [1] P. Coleman, *Introduction to Many-Body Physics*, (Cambridge University Press, Cambridge, United Kingdom, 2015).
- [2] B. C. Paul and K. Ingersent, arXiv:cond-mat/9607190 (1996).
- [3] B. C. Paul, *A study of a three-impurity Kondo model*, Ph.D. thesis, University of Florida, 2000.
- [4] K. Ingersent, A. W. W. Ludwig, and I. Affleck, Phys. Rev. Lett. **95**, 257204 (2005).